PHYSICS OF FLUIDS **28**, 032102 (2016)

Wave blocking phenomenon of surface waves on a shear flow with a constant vorticity

Philippe Maïssa,[1] Germain Rousseaux,[2] and Yury Stepanyants[3,a)]
[1]*Université de Nice-Sophia Antipolis, Laboratoire J.-A. Dieudonné, UMR CNRS-UNS 7351, Parc Valrose, 06108 Nice Cedex 02, France, European Union*
[2]*Institut Pprime, UPR 3346, CNRS — Université de Poitiers — ISAE ENSMA, 11 Bd Marie et Pierre Curie, BP 30179, 86962 Futuroscope, France, European Union*
[3]*Faculty of Health, Engineering and Sciences, University of Southern Queensland, Toowoomba, QLD 4350, Australia*

(Received 28 July 2015; accepted 27 December 2015; published online 1 March 2016)

Propagation of gravity-capillary surface waves on a background shear flow with a constant vorticity is studied and compared with the case when the background flow is uniform in depth. Under the assumption that the background flow gradually varies in the horizontal direction, the primary attention is paid to the wave blocking phenomenon; the effect of vorticity on this phenomenon is studied in detail. The conditions for wave blocking are obtained and categorized for different values of the governing dimensionless parameters: Froude number, dimensionless vorticity, and surface tension. © *2016 AIP Publishing LLC.* [http://dx.doi.org/10.1063/1.4942116]

I. INTRODUCTION

In many cases water waves propagate in moving water which leads to the complex phenomena of wave-current interaction. Usually, currents are nonuniform both in the vertical and horizontal directions. Many examples of wave propagation on the background of spatially nonuniform shear flows may be listed in conjunction with this phenomenon. Among them there are tidal currents, currents caused by wind stress, oceanic currents of different scales, currents induced by long surface or internal waves, river flows, etc. It is well-known that the interaction of water waves with nonuniform currents may result in either dramatic effects such as generation of freak waves[18,20] or favorable effects such as the blocking of waves by pneumatic wave-breakers.[38]

Due to the effect of friction at the sea bed and/or of wind stress at the free surface, the currents often vary with the depth. The result of such vertical flow variation is the presence of vorticity which plays an important role in the shear flow stability. The vorticity also gives rise to existence of specific vorticity waves which may exist not only in the interface of two layers of different vorticity, but even inside the shear flow with the continuously distributed vorticity (see, e.g., Ref. 32). Thus, the shear-flow vorticity in combination with the intensity of a current introduces an important parameter which should be taken into account in the attempts to understand the physics of the wave-current interaction. Leaving aside numerous works on the influence of shear flows on the stability of internal waves in a density stratified fluid, we only refer here to some papers where the interaction of surface waves with currents has been studied in the context of our study[3–5,7–14,17,21,24,31,34,39,40,42] (there is a plethora of publications in this field too; therefore, we are forced to restrict ourselves to those references which are most relevant to our work).

Here, we revisit the problem of wave-current interaction on a horizontally varying shear flow following the dynamical system approach.[23,30] We focus on the simplest case of a shear flow with the linear vertical profile having a constant vorticity; the more general case will be treated elsewhere. We show that the problem can be analyzed in terms of dimensionless parameters and introduce the "effective" Froude number defined such that the flow vorticity is taken into account

a)Author to whom correspondence should be addressed. Electronic mail: Yury.Stepanyants@usq.edu.au

along with the speed of the current. In the first part of this paper we consider pure gravity waves, but then, in the second part, we take into account the surface tension and show that, in addition to the known dimensionless parameters characterizing the wave-current interaction, the new length and velocity scales can be introduced in the context of the water wave theory through the balance of the effects of vorticity and surface tension.

We show also that due to specific properties of the water-wave dispersion, potentially unstable waves with negative energy can appear on a shear flow providing nontrivial features of wave blocking.

II. THE BLOCKING PHENOMENON OF SURFACE GRAVITY WAVES ON A CURRENT SLOWLY VARYING IN THE HORIZONTAL DIRECTION

Let us consider one-dimensional wave propagation on a surface of moving water of finite depth h. The velocity profile of the water flow $U(z)$ may be a rather complicated function of depth, but in this paper we focus on the consideration and intercomparison of two cases, (i) when the flow is depth independent but slowly varying in x: $U(x,z) = U_0(x)$ and (ii) when it is a linear function of depth $U(x,z) = U_0(x) + \alpha(x)z$. Here U_0 is the water speed at the free surface, and α characterizes the vorticity of the background flow. It is assumed that the z-axis is directed upward with zero at the unperturbed water surface. For definiteness, we suppose that $U_0 > 0$, i.e., we assume that the background flow is co-directed with the axis x. A sketch of the considered flow is shown in Fig. 1.

When the shear velocity is uniform in the horizontal direction but is an arbitrary function of z, the dispersion relation between the frequency ω and wave number k for waves of infinitesimal amplitude can be derived in the approximate form based on the Taylor series representation (see, e.g., Refs. 17, 34, and 37). However, recently it was found[16] that in many particular cases the dispersion relation can be presented in an explicit analytical form. Two simple cases of analytical representation of the dispersion relation in the closed form are very well known, they are those which have been mentioned above and shown in Fig. 1, i.e., when the velocity profile is either depth independent or varies linearly with the depth (in the former case the flow vorticity is zero, whereas in the latter case the flow vorticity is a constant). These two profiles were chosen for the analysis of the vorticity influence on the wave-current interaction and comparison of results obtained will be presented below.

Note that when the fluid velocity vanishes at the bottom (see Fig. 1), then $\alpha = U_0/h$, but in general α may be an independent parameter, in particular, putting $\alpha = 0$ we obtain the uniform current without vorticity. The shear flow vorticity can be controlled in the finite depth fluid with the help of a movable bottom, for example, using a rubber conveyor.

The dispersion relation for surface gravity waves in the linearly varying current was first derived by Thompson and Biesel[3,40] but has been re-derived in many papers both without and with the surface tension effect (see, e.g., Refs. 7, 9, 14, 31, 42, and 43). In the latter case it can be presented in the following explicit form in terms of the dependence of wave frequency ω on the

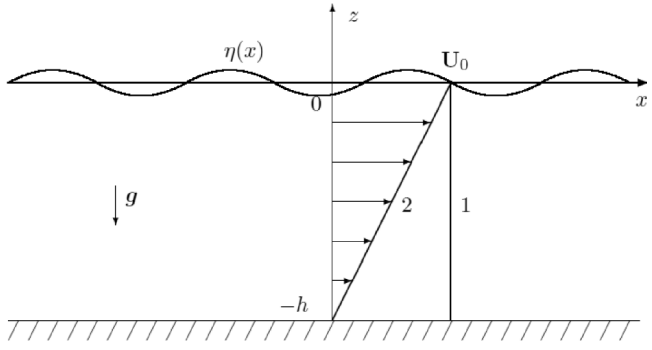

FIG. 1. Sketch of the fluid flow in the reference coordinate frame associated with the immovable bottom. Line 1 depicts the velocity with the uniform profile and line 2—the velocity with the linear profile.

wave number k of infinitesimal perturbations:

$$\omega^{\pm} = \mathbf{U}\cdot\mathbf{k}\left(1-\frac{\alpha}{2}\frac{\tanh|k|h}{U_0|k|}\right)+\sqrt{\left(\frac{\alpha}{2}\tanh|k|h\right)^2+(g+\sigma k^2)|k|\tanh|k|h}, \tag{1}$$

where g is the acceleration due to gravity, $\sigma=\gamma/\rho$ is the normalised coefficient of surface tension, and ρ is the water density. Here we assume that the physical frequency is a positive quantity $\omega = 2\pi/T$, where T is the wave period, and the wave number k may be of either sign.

The dispersion relation consists of two branches designated by upper indices plus and minus; index plus pertains to co-current propagating waves with $k>0$, and index minus to counter-current propagating waves with $k<0$. Note that the frequency may formally become negative at certain conditions for counter-current propagating waves with $k<0$. In such cases using the invariance of the phase speed $c_p \equiv \omega/k$ under the transformation $\omega\to-\omega$, $k\to-k$, the negative portion of the dispersion curve with $\omega<0$ can be transferred to the domain where $\omega>0$ and $k>0$.

By introducing the normalized variables, $\kappa = kh$ and $\tilde{\omega}=\omega\sqrt{h/g}$, we can present Eq. (1) in the dimensionless form

$$\tilde{\omega}^{\pm} = \left(\hat{\mathbf{U}}_0\cdot\hat{\mathbf{k}}_0\right)(\mathrm{Fr}\,|\kappa|-\Omega\tanh|\kappa|)+\sqrt{(\Omega\tanh|\kappa|)^2+(1+\mathrm{S}\kappa^2)|\kappa|\tanh|\kappa|}, \tag{2}$$

where $\mathrm{Fr}=U_0/\sqrt{gh}$ is the Froude number, $\Omega=\alpha h/(2\sqrt{gh})$ is the normalised vorticity parameter, $\mathrm{S}=\sigma/\left(gh^2\right)$ is the parameter which measures the strength of the capillary effect relative to the gravity effect, and $\hat{\mathbf{U}}_0$ and $\hat{\mathbf{k}}_0$ are the unit vectors in the direction of the flow velocity and wave number, respectively.

Note that in some cases it may be convenient to introduce the "effective" Froude number defined such that the flow vorticity Ω is taken into account: $\mathrm{F}_\Omega=(\mathrm{Fr}-\Omega)(1+\Omega^2)^{-1/2}$. If the background flow is uniform with depth ($\Omega=0$), then the effective Froude number reduces to the conventional Froude number Fr defined above. If the background flow has a linear profile vanishing at the bottom as shown in Fig. 1 (the constant vorticity flow), then $\Omega=\mathrm{Fr}/2$ and $\mathrm{F}_\Omega=\mathrm{Fr}/\sqrt{4+\mathrm{Fr}^2}$. The effect of introducing the new form of the Froude number is especially clear when we consider the limiting case of gravity waves in shallow water; then dispersion relation (1) reduces to

$$\omega^{\pm}(k)|_{k\to0} = \pm\left(U_0-\frac{\alpha h}{2}\right)|k|+|k|\sqrt{\left(\frac{\alpha h}{2}\right)^2+gh}. \tag{3}$$

In this case one can introduce the "effective" uniform velocity $\bar{U}=U_0-\alpha h/2$ and speed of long waves $\bar{c}=\sqrt{(\alpha h/2)^2+gh}$. Then the "effective" Froude number can be defined in the traditional manner,

$$\mathrm{F}_\Omega=\frac{\bar{U}}{\bar{c}}=\frac{U_0-\alpha h/2}{\sqrt{(\alpha h/2)^2+gh}}=\frac{\mathrm{Fr}-\Omega}{\sqrt{1+\Omega^2}}. \tag{4}$$

In what follows, we consider the propagation of a quasi-sinusoidal wavetrain with a fixed frequency assuming that the current velocity and vorticity vary smoothly in the horizontal direction so that the characteristic scale of current variation L is much greater than the characteristic wavelength of the wavetrain $\lambda=2\pi/|k|$. In this case, the frequency of the wave train remains constant, whereas its wavenumber adiabatically varies in space in accordance with the flow variation. To determine the character of the spacial variation of the carrier wavenumber we need to present dispersion equation (2) in terms of $\kappa[\tilde{\omega},\mathrm{Fr}(x)]$ assuming that the wave frequency is fixed. Unfortunately, such a solution cannot be presented in explicit analytical form for a fluid of arbitrary depth; however, it can be obtained in the limiting cases of deep and shallow water when $|\kappa|\gg1$ or $|\kappa|\ll1$, respectively. Nevertheless, some interesting features of wave motion can be derived even for an arbitrary constant depth. Below we first discuss propagation of pure gravity waves in a spatially varying shear flow, and then we take into account the surface tension effect.

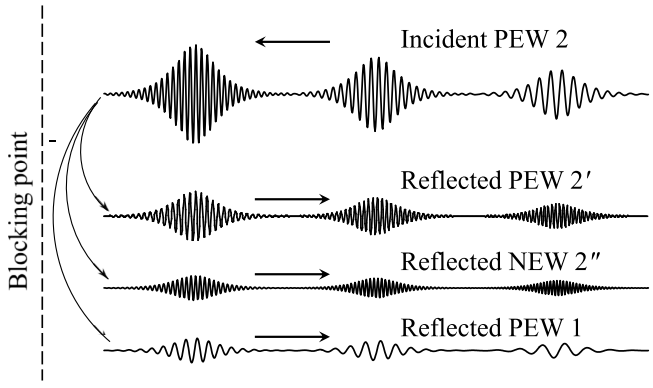

FIG. 2. Schematic illustration of wave blocking phenomenon for pure gravity waves (the plot is not to scale).

A. The wave blocking of gravity waves in a fluid of arbitrary depth

If a wavetrain propagates against a gradually increasing current, the group velocity of the wavetrain $\tilde{c}_g \equiv d\tilde{\omega}/d\kappa$ decreases as the wavetrain is decelerated by the current. When the current becomes so strong that the group velocity vanishes, then the "*wave blocking phenomenon*" occurs (see, e.g., Ref. 27). There is a plethora of papers and books devoted to this phenomenon; it is not possible to list all of them in this paper; therefore, we refer only to some of them in the text when necessary.

Figure 2 illustrates schematically the blocking phenomenon for pure gravity waves with subsequent generation of reflected waves at the blocking point. In the geometry considered here, the incident wave denoted by number 2 has negative group and phase velocities; it propagates to the left against the current. All reflected waves have positive group velocities, but their phase velocities are different. For the first of them, denoted by 2′, the phase velocity is negative, whereas for the other reflected waves 1 and 2″, the phase velocities are positive.

It can be shown that the energy of one of the reflected waves is negative, whereas all other waves possess positive energy. The general concept of negative energy waves (NEWs) has been discussed in many publications, see, for example, Refs. 2, 6, 15, 22, 25, 26, 31, and 36. The basic idea of this concept is that the total energy of a medium with the excited wave is less than without the wave, whereas in the usual case of positive energy waves (PEWs) the total energy of a medium with the wave is greater than without the wave. In Fig. 2 the positive and negative energy waves are indicated.

As has been mentioned above, the condition for the wave blocking phenomenon is the vanishing of the group speed of a wavetrain. Differentiating dispersion relation (2) (with S = 0) with respect to κ and setting $d\tilde{\omega}/d\kappa = 0$, we obtain the following equation for the blocking of counter-propagating waves ($\kappa < 0$):

$$\left(2\Omega^2 \tanh\kappa + \kappa\right)\left(1 - \tanh^2\kappa\right) + \tanh\kappa + 2\left[\mathrm{Fr} - \Omega\left(1 - \tanh^2\kappa\right)\right]\sqrt{\Omega^2\tanh^2\kappa + \kappa\tanh\kappa} = 0. \tag{5}$$

The critical wave number corresponding to the blocking phenomenon follows from this transcendental equation for the given values of Fr and Ω. However, this equation can be readily solved with respect to Fr; by solving it one finds the critical Froude number Fr_b for which wavetrains with carrier wavenumbers $\kappa < \kappa_b$ will be blocked, where κ_b is the root of Eq. (5),

$$\mathrm{Fr}_b = \frac{1}{\cosh^2\kappa_b}\left[\Omega - \frac{2\left(\kappa_b + 2\Omega^2\tanh\kappa_b\right) + \sinh 2\kappa_b}{4\sqrt{\tanh\kappa_b\left(\kappa_b + \Omega^2\tanh\kappa_b\right)}}\right]. \tag{6}$$

This dependence is illustrated by Fig. 3 which shows the blocking wavenumber κ_b against the corresponding Froude number Fr_b at different vorticity parameters Ω. In particular, the horizontal dashed line shows that the wavetrains with $|\kappa_b| > 1$ can be blocked by the Froude number which is greater than the value at the intersection with line 1, if Ω = 0, or at the intersection with line 2, if Ω = 0.5, or at the intersection with line 3 if Ω = 1. Thus, the higher the vorticity, the higher value of the Froude number is required to block a wavetrain with a certain wavenumber.

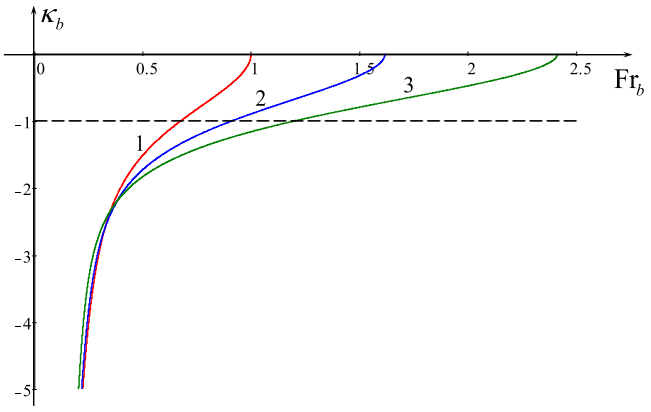

FIG. 3. The dependence of the blocking wavenumber κ_b against the critical Froude number Fr_b at different vorticity parameters Ω. Line 1—$\Omega = 0$, line 2—$\Omega = 0.5$, line 3—$\Omega = 1$.

The corresponding blocking frequency $\tilde{\omega}_b(\mathrm{Fr}_b)$ can be presented in parametric form if one substitutes Eq. (6) into dispersion equation (2) with S = 0 for counter-current propagating waves,

$$\tilde{\omega}_b = \left(\tanh\kappa_b - \frac{\kappa_b}{\cosh^2\kappa_b}\right)\left[\frac{\kappa_b + 2\Omega^2\tanh\kappa_b}{2\sqrt{\tanh\kappa_b\,(\kappa_b + \Omega^2\tanh\kappa_b)}} - \Omega\right]. \tag{7}$$

The relationship between the frequency of the blocked wave and Froude number can be also presented in terms of the parametric dependence of critical Froude number on the normalized wave period $\tilde{T}_b \equiv T_b\sqrt{g/h}$,

$$\mathrm{Fr}_b = \mathrm{Fr}\,(\kappa_b, \Omega), \qquad \tilde{T}_b = \frac{2\pi}{\tilde{\omega}_b(\kappa_b, \Omega)}, \tag{8}$$

where Eqs. (6) and (7) should be used for $\mathrm{Fr}\,(\kappa_b, \Omega)$ and $\tilde{\omega}_b(\kappa_b, \Omega)$. The dependence $\mathrm{Fr}_b(\tilde{T}_b)$ is shown in Fig. 4 for the same three values of Ω as in Fig. 3.

In the limiting cases of deep and shallow water the corresponding dependences can be derived explicitly (see Subsections II B and II C).

B. Gravity wave blocking in deep water

Within the framework of the deep-water approximation, $|\kappa| \gg 1$, dispersion relation (2) for $\kappa < 0$ can be presented as the following quadratic polynomial in κ:

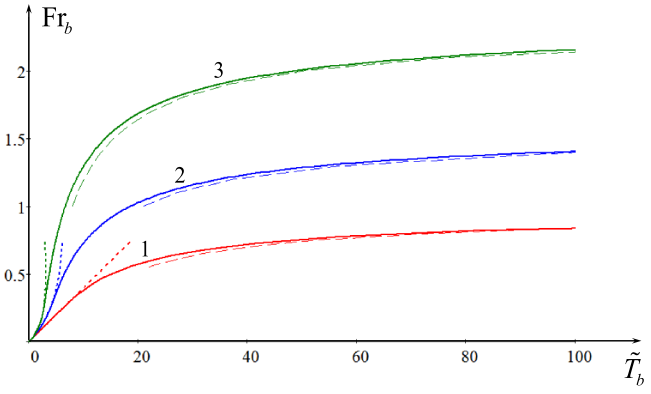

FIG. 4. The dependence of critical Froude number against the wave period $\tilde{T}_b$. Line 1—$\Omega = 0$, line 2—$\Omega = 0.5$, line 3—$\Omega = 1$. Dotted lines pertain to asymptotic dependences for small periods, whereas dashed lines pertain to asymptotic dependences for large periods.

$$\mathrm{Fr}^2\kappa^2 + [2\mathrm{Fr}\,(\tilde{\omega} - \Omega) - 1]\,|\kappa| + \tilde{\omega}(\tilde{\omega} - 2\Omega) = 0. \tag{9}$$

To normalise the wavenumber one can use instead of water depth h the initial value of the carrier wave length λ_0 chosen at a certain reference point x_0.

As already mentioned, the condition for the wave blocking phenomenon is the vanishing of the group speed of a wavetrain. This corresponds to the situation when the discriminant of quadratic Eq. (9) is exactly zero, and the two roots of this equation coincide.[23,30] Under this condition dispersion relation (9) can be presented in the factorized form

$$(\kappa - \kappa_b)^2 = 0, \quad \text{where} \quad \kappa_b = -\frac{1 - 2\mathrm{Fr}_b\,(\tilde{\omega}_b - \Omega)}{2\mathrm{Fr}_b^2}. \tag{10}$$

The corresponding value of the frequency when the discriminant vanishes is

$$\tilde{\omega}_b = \frac{1}{4\mathrm{Fr}_b} + \Omega\,(1 + \mathrm{Fr}_b\,\Omega)\,. \tag{11}$$

Using this equation, one can eliminate $\tilde{\omega}$ from the expression for κ_b in Eq. (10) and present it in the alternative form:

$$\kappa_b = \Omega^2 - \frac{1}{4\mathrm{Fr}_b^2}. \tag{12}$$

In the absence of vorticity, when $\Omega = 0$, the normalized frequency, $\tilde{\omega}_b$, as per Eq. (11), monotonically decreases with the Froude number. But when the vorticity parameter is non-zero, the dependence $\tilde{\omega}_b(\mathrm{Fr}_b)$ formally becomes non-monotonic, attaining a minimum value at $\mathrm{Fr}_b = 1/2\Omega$. However, the non-monotonic behavior of $\tilde{\omega}_b(\mathrm{Fr}_b)$ is actually just an artefact of the deep-water approximation ($|\kappa| \gg 1$), which is valid only when $\mathrm{Fr}_b \ll 1$.

Dependence (11) can also be presented in the form of a relationship between the critical Froude number Fr_b and normalized wave period $\tilde{T}_b$ similar to Eq. (8), but in the explicit form

$$\tilde{T}_b(\mathrm{Fr}, \Omega) = \frac{8\pi\mathrm{Fr}_b}{(1 + 2\Omega\mathrm{Fr}_b)^2}. \tag{13}$$

The inverse dependence $\mathrm{Fr}(\tilde{T}_b)$ is shown in Fig. 4 by dotted lines for the corresponding values of Ω.

As one can see from this figure, the deep-water approximation is valid in the range of relatively small wave periods and small Froude numbers. In the limit $\tilde{T}_b \to 0$ we have a universal linear dependence $\mathrm{Fr}_b = \tilde{T}_b/(8\pi)$ regardless of Ω. The linear dependence between the Froude number and wave period for very short gravity waves blocked by a *uniform current* with $\Omega = 0$ has been derived in Refs. 23 and 30. Here we have found that for the shear flow with a linear profile (constant vorticity flow) exactly the same linear dependence between these quantities occurs.

C. Gravity wave blocking in shallow water

For the sake of completeness, consider also another limiting case $|\kappa| \ll 1$, $\kappa < 0$, which corresponds to the shallow-water approximation. In this case dispersion relation (2) reads

$$\tilde{\omega} \approx -\left(\Omega + \sqrt{1 + \Omega^2} - \mathrm{Fr}\right)\kappa + \left(\Omega + \frac{1 + 2\Omega^2}{2\sqrt{1 + \Omega^2}}\right)\frac{\kappa^3}{3} + o(\kappa^3). \tag{14}$$

From the condition of wave blocking, $d\tilde{\omega}/d\kappa = 0$ we obtain

$$\kappa_b(\mathrm{Fr}_b, \Omega) = -\frac{\sqrt{2\sqrt{1 + \Omega^2}\left(\Omega + \sqrt{1 + \Omega^2} - \mathrm{Fr}_b\right)}}{\Omega + \sqrt{1 + \Omega^2}}, \tag{15}$$

$$\tilde{\omega}_b(\mathrm{Fr}_b, \Omega) = -\frac{2}{3}\kappa_b(\mathrm{Fr}_b, \Omega)\frac{\Omega\left(3 + 4\Omega^2\right) + \left(1 + 4\Omega^2\right)\sqrt{1 + \Omega^2} - \left(\Omega + \sqrt{1 + \Omega^2}\right)^2\mathrm{Fr}_b}{\left(\Omega + \sqrt{1 + \Omega^2}\right)^2}. \tag{16}$$

In the particular case of a uniform flow, $\Omega = 0$, these expressions reduce to

$$\kappa_b(\mathrm{Fr}_b, 0) = -\sqrt{2(1-\mathrm{Fr}_b)}, \quad \tilde{\omega}_b(\mathrm{Fr}_b, 0) = \frac{2\sqrt{2}}{3}(1-\mathrm{Fr}_b)^{3/2}. \tag{17}$$

The dependence $\tilde{\omega}_b(\mathrm{Fr}_b, \Omega)$ can also be presented in the form of a relationship between the critical Froude number and the dimensionless period $\tilde{T}_b$ of the blocked wave,

$$\tilde{T}_b(\mathrm{Fr}_b, \Omega) = \frac{3\pi\sqrt{2}}{2} \frac{\Omega + \sqrt{1+\Omega^2}}{(1+\Omega^2)^{1/4}\left(\Omega + \sqrt{1+\Omega^2} - \mathrm{Fr}_b\right)^{3/2}} \quad \text{and} \quad \tilde{T}_b(\mathrm{Fr}_b, 0) = \frac{3\pi\sqrt{2}}{2(1-\mathrm{Fr}_b)^{3/2}}. \tag{18}$$

These dependences are shown in Fig. 4 by dashed lines for large values of $\tilde{T}_b$, as they are only asymptotically valid at very large wave periods (i.e., at small wave numbers $|\kappa| \ll 1$).

It is clearly seen from Eq. (18) that when $\mathrm{Fr}_b \to \mathrm{Fr}_\infty \equiv \Omega + \sqrt{1+\Omega^2}$, then the wave period goes to infinity, and when the Froude number exceeds Fr_∞, then waves of any period are blocked, i.e., they cannot propagate over the blocking point. The critical Froude number is equal to one for the uniform current and increases with the vorticity parameter Ω. Physically this is quite understandable. Indeed, the wave motion induced by a surface wave decays with the depth (see, e.g., Ref. 19). The characteristic scale of decay depends on the wavelength, which, in turn, depends through the dispersion relation on the wave period. The larger the period, the larger the characteristic vertical scale of the wave motion. When $\Omega \neq 0$, the current velocity linearly decreases with the water depth; therefore, its influence on the wave gradually decreases and vanishes at the bottom. On the other hand, when the flow vorticity is zero, $\Omega = 0$, then the current uniformly affects a wave at any depth.

III. THE INFLUENCE OF SURFACE TENSION ON THE BLOCKING PHENOMENON

Surface tension drastically affects the blocking phenomenon in the range of relatively short gravity-capillary waves. To demonstrate this we return to dispersion relation (2). Short-period waves are usually associated with the deep-water approximation $|\kappa| \gg 1$ which allows one to replace $\tanh|\kappa|$ by 1 in Eq. (2). The deep-water approximation is used below where possible to simplify the analytical treatment, but the exact formulae are used when the deep-water approximation fails.

The plots of dispersion relation (2) for the counter-current propagating waves $\tilde{\omega}^-(\kappa)$ are shown in Fig. 5 for several values of Froude number and fixed parameters $\Omega = 0$ and $S = 7.4 \times 10^{-6}$. This choice of parameters corresponds to uniform water flow in a reservoir of 1 m depth with surface tension $\gamma = 0.073$ N/m. The plots remain qualitatively the same for $\Omega \neq 0$ and only slightly change quantitatively.

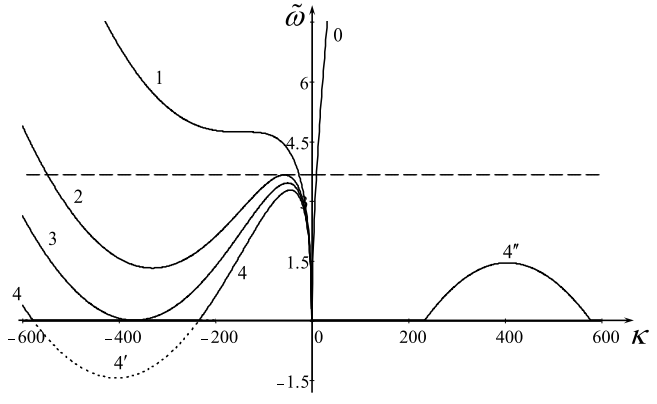

FIG. 5. Dimensionless frequency of upstream and downstream (line 0) propagating waves as a function of the dimensionless wavenumber as per Eq. (2) with $\Omega = 0$ and $S = 7.4 \times 10^{-6}$. Lines 0 and 1 pertain to $\mathrm{Fr} = 5.67 \times 10^{-2}$, line 2—$\mathrm{Fr} = 7.0 \times 10^{-2}$, line 3—$\mathrm{Fr} = \mathrm{Fr}_{NEW} \equiv \sqrt[4]{4S}$, lines 4, 4′, and 4″ pertain to $\mathrm{Fr} = 7.75 \times 10^{-2}$.

A. A condition for wave blocking

When the Froude number is zero or sufficiently small, the dispersion curve is monotonic as shown by line 1 in the figure. As long as the dispersion curve is monotonic, there are no blocked waves in the flow; they appear when the group speed turns to zero, $\tilde{c}_g \equiv d\tilde{\omega}^-/d\kappa = 0$, i.e., when an inflection point appears on the curve $\tilde{\omega}^-$ (as Fr increases further, the inflection point splits into two extrema — one local maximum and one local minimum). This occurs when the Froude number exceeds a certain critical value $\mathrm{Fr}_{in}(\Omega, \mathrm{S})$ which can be found in the deep-water approximation from the equation

$$\mathrm{Fr}_{in}^8 + 18\,\mathrm{S}\,\mathrm{Fr}_{in}^4 + 108\,\mathrm{S}^2\Omega^2\mathrm{Fr}_{in}^2 - 27\,\mathrm{S}^2 = 0. \tag{19}$$

When the minimal Froude number is determined from Eq. (19) for the given parameters Ω and S, then the critical wave number and frequency which give birth to two extrema in the dispersion curve $\tilde{\omega}^-(\kappa)$ can be found from the following formulae:

$$\kappa_{in}(\Omega, \mathrm{S}) = -\frac{\mathrm{Fr}_{in}^2}{3\mathrm{S}}, \quad \tilde{\omega}_{in}(\Omega, \mathrm{S}) = \frac{1}{6\mathrm{S}\,\mathrm{Fr}_{cr}}\left(3\mathrm{S} - \mathrm{Fr}_{in}^4 + \sqrt{9\mathrm{S}^2 - 6\mathrm{S}\mathrm{Fr}_{in}^4 - \mathrm{Fr}_{in}^8/3}\right). \tag{20}$$

In the case of a uniform flow, Ω = 0, all critical parameters can be written explicitly,

$$\mathrm{Fr}_{in}(0, \mathrm{S}) = \sqrt[4]{3\mathrm{S}\left(2\sqrt{3} - 3\right)}, \quad \kappa_{in}(0, \mathrm{S}) = -\sqrt{\frac{2\sqrt{3} - 3}{3\mathrm{S}}}, \quad \tilde{\omega}_{in}(0, \mathrm{S}) = \sqrt[4]{\frac{\left(2\sqrt{3} - 3\right)^3}{27\mathrm{S}}}. \tag{21}$$

These non-dimensional quantities can be presented in the dimensional form for the velocity, wave number, and frequency, respectively (cf. Ref. 30),

$$U_c = \frac{\sqrt{3}}{\left(3 + 2\sqrt{3}\right)^{\frac{1}{4}}}\sqrt{\frac{g}{K}}, \quad k_c = \frac{K}{\left(3 + 2\sqrt{3}\right)^{\frac{1}{2}}}, \quad \omega_c = \frac{2\pi}{T_c} = \frac{\sqrt{gK}}{\left(3 + 2\sqrt{3}\right)^{\frac{3}{4}}}, \tag{22}$$

where $K = \sqrt{g/\sigma}$.

The critical Froude number monotonically increases with S, whereas the critical wave number and frequency decrease with S. The analysis of Eqs. (19) and (20) shows that the dependences of Fr_{in} and κ_{in} on Ω are very weak, at least for the realistically small values of the parameter $\mathrm{S} \sim 10^{-5}$, whereas its influence on $\tilde{\omega}_{in}$ is small, but noticeable. In the case of clean water, the largest value of the parameter $\mathrm{S} = 10^{-2}$ can be attained for the fluid depth $h \approx 2.7$ cm. (Note that in a deep basin with a near-surface current a gradient of the linear shear flow may be much stronger than U_0/h; then the influence of the parameter Ω may be quite noticeable.)

The typical form of the dispersion curve for $\mathrm{Fr} > \mathrm{Fr}_{in}$ is shown by line 2 in Fig. 5. The local maximum on the curve corresponds to the first blocking point, when the incoming wave train stops and turns back with continuously increasing wave number.[33,41] The higher the current speed (the higher the Froude number), the smaller the frequency of the blocked wave train.

The local minimum on the dispersion curve corresponds to the second blocking point, when the wave train reflected from the first blocking point travels downstream, reflects again at a certain point and propagates upstream. Below we discuss qualitatively these transformations in more detail. Some aspects of wave transformation at the blocking points have been studied experimentally,[1,28] analytically and numerically in Ref. 41.

Let us assume that a wavetrain (the incident gravity wave) of carrier frequency $\tilde{\omega}_0$ (depicted by dashed line in Fig. 5) propagates against a sufficiently strong current capable of blocking the wavetrain at some point. If initially the wavetrain is propagating in the region where the dispersion curve is monotonic, like line 1 in Fig. 5, it eventually attains the point where the dispersion curve has a maximum (see the transition from line 1 to line 2 along the horizontal dashed line in Fig. 5). Then it stops (because its group velocity at the maximum of the dispersion curve vanishes) and transfers into other waves which propagate away from the blocking point. Two of these waves are reflected. One of them is a gravity-capillary wave on the same branch of the dispersion curve $\tilde{\omega}^-(\kappa)$, but on the other side of the maximum of dispersion curve; its wave number is greater in absolute

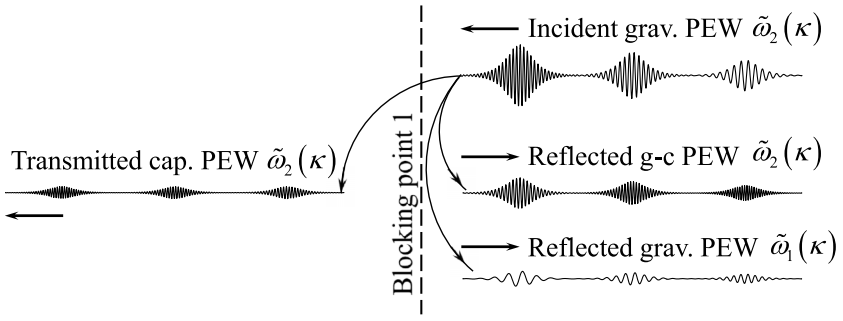

FIG. 6. Schematic illustration of one of the scenarios of blocking phenomenon for gravity-capillary waves. The incident wave gives rise to two reflected waves and one transmitted wave.

value than the wave number of the incident wave. When this wave propagates with the stream, its wave number increases in absolute value. The group velocity of this wave is positive and the energy flux is co-directed with the current, whereas its phase velocity remains negative.

Another reflected gravity wave is the co-current propagating wave, which lies on the dispersion curve $\tilde{\omega}^+(\kappa)$ (see line 0 in Fig. 5 where it intersects with the dashed line). This wave propagates to the right having positive group and phase velocities with gradually increasing wave number.

In addition to this, there is a pure capillary transmitted wave generated at the blocking point on the dispersion curve $\tilde{\omega}^-(\kappa)$. This wave propagates against the current with increasing wave number (in absolute value) and having negative group and phase velocities.

This transformation is schematically shown in Fig. 6. All waves are of positive energy and of the same frequency $\tilde{\omega}_0$.

B. Secondary wave blocking

The gravity wave $\tilde{\omega}^+(\kappa)$ and capillary wave $\tilde{\omega}^-(\kappa)$ propagate to plus and minus infinity, respectively, without further reflections, whereas the fate of the reflected gravity-capillary wave $\tilde{\omega}^-(\kappa)$ is more complicated. When it propagates downstream, it experiences gradual change of its wavenumber because the dispersion curve also adiabatically changes such that its local minimum eventually attains the value $\tilde{\omega}_0$. At this moment the second blocking point arises. Now this gravity-capillary wave becomes the incident wave $\tilde{\omega}^-(\kappa)$ giving rise to two reflected waves (one of them is conditionally a gravity wave $\tilde{\omega}^-(\kappa)$ and the other is a capillary wave $\tilde{\omega}^-(\kappa)$) and one transmitted gravity wave $\tilde{\omega}^+(\kappa)$ as illustrated by Fig. 7.

The gravity wave $\tilde{\omega}^+(\kappa)$ and capillary wave $\tilde{\omega}^-(\kappa)$ propagate again to plus and minus infinity, respectively, without further reflections, whereas the other gravity wave $\tilde{\omega}^-(\kappa)$ propagates against the stream and experiences the same transformation as already described and illustrated in Fig. 6. Then, the process of transformation of gravity-capillary and pure gravity waves on the dispersion curve $\tilde{\omega}^-(\kappa)$ repeats many times.

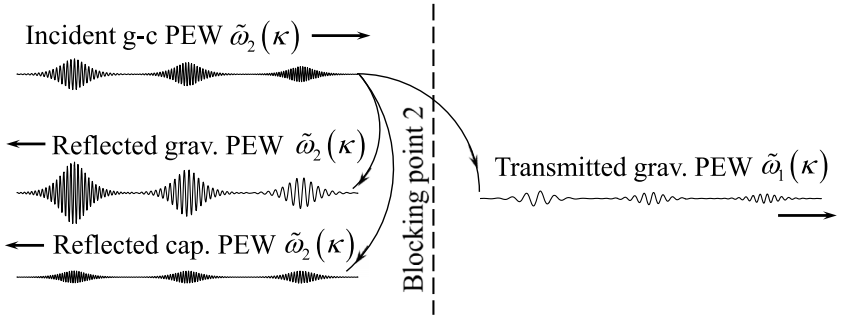

FIG. 7. Secondary transformation of reflected gravity-capillary wave $\tilde{\omega}^-(\kappa)$ shown in the previous figure.

Thus, in the considered case we deal with a specific kind of resonator for the wavetrain locked in between two spatially separated blocking points 1 and 2. The wavetrain experiences energy loses through the leaking boundaries of the resonator at each reflection.

C. Negative energy waves

When the Froude number further increases and exceeds a certain critical value

$$\mathrm{Fr}_c(\kappa_m, \Omega, \mathrm{S}) = \sqrt{\left(1 + \mathrm{S}\kappa_m^2 + \Omega^2 \frac{\tanh|\kappa_m|}{|\kappa_m|}\right) \frac{\tanh|\kappa_m|}{|\kappa_m|}}, \tag{23}$$

then the wave frequency at the minimum becomes less than $\tilde{\omega}_c^- = \Omega \tanh|\kappa_m|$. As has been shown in our paper,[31] in this case negative energy waves (NEWs) appear in the system. The expressions for k_m and Fr_c cannot generally be presented in analytic form, but in the deep-water approximation the corresponding expressions will be given below. Notice that in the presence of vorticity NEWs appear even at positive frequencies $\tilde{\omega}^- < \tilde{\omega}_c^-$, whereas in the uniform flow with $\Omega = 0$ the condition for the appearing NEWs is $\tilde{\omega}^- < 0$ (cf. Refs. 35 and 36).

If the surface tension is neglected, then NEWs exist in the flow for any $\mathrm{Fr} > 0$ in the range of wavenumbers $-\infty < \kappa < \kappa_c$, where κ_c is the root of the transcendental equation for the given parameters Ω and Fr,

$$\frac{\tanh|\kappa_c|}{|\kappa_c|} = \frac{\sqrt{1 + 4\Omega^2\mathrm{Fr}^2} - 1}{2\Omega^2}. \tag{24}$$

As follows from this formula, surface waves of any wavenumber become NEWs when $\mathrm{Fr} > \sqrt{1 + \Omega^2}$. In deep-water approximation Eq. (24) gives

$$\kappa_c = -\frac{\sqrt{1 + 4\Omega^2\mathrm{Fr}^2} + 1}{2\mathrm{Fr}^2}. \tag{25}$$

When the surface tension is taken into account, then NEWs appear only when the Froude number is greater than the critical value as per Eq. (23) and they exist only in a finite range of wavenumbers. As mentioned above, the minimum value of critical Froude number (23) can be found in analytic form in the deep-water approximation; the corresponding wavenumber in this case is

$$\kappa_m = -\frac{1}{\mathrm{S}} \sqrt[3]{\mathrm{S}^2\Omega^2 K_m} - \frac{1}{3\sqrt[3]{\mathrm{S}^2\Omega^2 K_m}}, \tag{26}$$

where $K_m = 1 + \sqrt{1 - (27\mathrm{S}\Omega^4)^{-1}}$, and the minimal Froude number is

$$\mathrm{Fr}_c = \frac{\sqrt[3]{\mathrm{S}\Omega\sqrt{K_m}}}{1 + 3\sqrt[3]{\mathrm{S}\Omega^4 K_m^2}} \sqrt{6 + 9\sqrt[3]{\mathrm{S}\Omega^4 K_m}\left(2\sqrt[3]{K_m} + 3\sqrt[3]{\mathrm{S}\Omega^4}\right)}. \tag{27}$$

In the case of a uniform flow ($\Omega = 0$) we obtain $\kappa_m = 1/\sqrt{\mathrm{S}}$, $\mathrm{Fr}_c = \sqrt[4]{4\mathrm{S}}$. (These quantities in the dimensional form correspond, respectively, to the wave number $k_{g\sigma} = \sqrt{g/\sigma}$ and velocity $U_{g\sigma} = \sqrt[4]{4g\sigma}$ obtained in Ref. 30 in the asymptotic limit when the wave period $T \to \infty$ ($\omega \to 0$).) It is remarkable that the threshold value of $\tilde{\omega}_c^-$ when NEWs appear at Fr_c is independent of S and simply equal to Ω: $\tilde{\omega}_c^-(\kappa_m) = \Omega$.

The details of direct calculations of wave energy for surface waves on a shear flow with a constant vorticity can be found in our paper.[31]

At even greater Froude numbers, $\mathrm{Fr} > \mathrm{Fr}_c$, the frequency $\tilde{\omega}^-$ in Eq. (2) formally becomes negative (see line 4 with the dashed portion 4′ in Fig. 5). From the kinematic point of view, waves with negative frequencies and negative wavenumbers are equivalent to waves with positive frequencies and positive wave numbers (see line 4″ in Fig. 5) as they have the same phase velocities.

Further increase of the Froude number leads to the decrease of the primary frequency maximum associated with PEWs (see line 4 in Fig. 5) and increase of the secondary frequency maximum

associated with NEWs (see line 4″ in Fig. 5). At a certain value of Froude number Fr_{eq}, the two frequency maxima for PEWs propagating upstream and NEWs propagating downstream become equal (this situation corresponds to the velocity U_b introduced in Ref. 30). At greater Froude numbers, the local maximum on the dispersion curve 4″ for NEWs becomes even greater than the local maximum of dispersion curve 4 for PEWs.

D. The relationship between the wave period and Froude number at the blocking points

The relationship between the wave frequencies at the blocking points $\tilde{\omega}_b^-$ (i.e., at the maximum and minimum of the dispersion curve $\tilde{\omega}^-$—see, e.g., line 2 in Fig. 5) and the Froude number Fr_b can be presented in parametric form. In the deep-water approximation the formulae read (recall that $\kappa < 0$)

$$\tilde{\omega}_b^-(\kappa,\Omega,\mathrm{S}) = \frac{|\kappa|\left(1-\mathrm{S}\kappa^2\right)+2\Omega\left(\Omega+\sqrt{|\kappa|\left(1+\mathrm{S}\kappa^2\right)+\Omega^2}\right)}{2\sqrt{|\kappa|\left(1+\mathrm{S}\kappa^2\right)+\Omega^2}}, \tag{28}$$

$$\mathrm{Fr}_b(\kappa,\Omega,\mathrm{S}) = \frac{1+3\mathrm{S}\kappa^2}{2\sqrt{|\kappa|\left(1+\mathrm{S}\kappa^2\right)+\Omega^2}}. \tag{29}$$

As has been mentioned above, when $\tilde{\omega}_b^-$ becomes negative in Eq. (28), we can change the sign of both $\tilde{\omega}_b^-$ and κ, then we obtain the NEWs branch of $\tilde{\omega}_b(\kappa)$ with positive κ (i.e., we undertake a jump from line 4′ to line 4″ in Fig. 5).

In the case of a uniform flow these formulae simplify and reduce to (cf. Ref. 29)

$$\tilde{\omega}_b^-(\kappa,0,\mathrm{S}) = \frac{\sqrt{|\kappa|}}{2}\frac{1-\mathrm{S}\kappa^2}{\sqrt{1+\mathrm{S}\kappa^2}}, \qquad \mathrm{Fr}_b(\kappa,0,\mathrm{S}) = \frac{1+3\mathrm{S}\kappa^2}{2\sqrt{|\kappa|\left(1+\mathrm{S}\kappa^2\right)}}. \tag{30}$$

In another limiting case, when the surface tension is neglected (S = 0), Eqs. (28) and (29) reduce to Eq. (11).

The relationship between $\tilde{\omega}_b^-$ and Fr_b can also be presented in terms of parametric dependence of the critical Froude number on the normalized wave period $\mathrm{Fr}_b\left(\tilde{T}_b\right)$, where $\tilde{T}_b = T_b\sqrt{g/h}$. This dependence is plotted in Fig. 8(a) for $\Omega = 0$ and in Fig. 8(b) for $\Omega = 1$ (a similar dependence is given by Eq. (8) for the case when the surface tension is neglected; it is presented in Fig. 4).

Dotted lines 1 in these figures pertain to the case of pure gravity waves without surface tension; they are the same as shown in Fig. 4 for the corresponding values of Ω. Lines 2 depict the dependence of the critical Froude number on the wave period for the first blocking point, which corresponds to the maximum of PEWs on the dispersion curve (see the maxima on the curves in the left half-plane of Fig. 5). These lines asymptotically approach the corresponding dotted lines 1 when the period increases and the influence of the surface tension diminishes.

Lines 2′ depict the dependence of the critical Froude number on the wave period for the second blocking point which corresponds to the minimum of PEWs on the dispersion curve (see the minima on the curves in the left half-plane of Fig. 5).

Lines 2″ depict the dependence of the critical Froude number on the wave period for the third blocking point which corresponds to the maximum of NEWs on the dispersion curve (see, e.g., the maximum on curve 4″ in the right half-plane of Fig. 5).

Dashed horizontal lines 3 indicates the critical Froude number as per Eq. (21) in the case of $\Omega = 0$ or per Eqs. (19) and (20) in general; below these lines the blocking phenomenon is impossible in the presence of surface tension. And dashed vertical lines 4 indicate the corresponding critical value of the wave period; waves with shorter periods cannot be blocked at any Froude number.

Dashed horizontal lines 3′ indicate the Froude number at which the frequency of the blocked wave $\tilde{\omega}_b^-$ vanishes (see Eq. (28) for the deep water case). In the case $\Omega = 0$ the corresponding value of the Froude number Fr_c is given after Eq. (27). When $\Omega \neq 0$, the asymptotic value of the Froude number cannot be presented by a simple formula in general, but its approximate value can be estimated for small Ω: $\mathrm{Fr}_b \approx \sqrt[4]{4\mathrm{S}}\left(1+\Omega\sqrt[4]{\mathrm{S}/4}\right)$. In the dimensional variables this gives

$$U_{g\sigma\alpha} \approx U_{g\sigma}\left(1+\frac{\alpha}{2\sqrt{2}}\sqrt[4]{\frac{\sigma}{g^3}}\right).$$

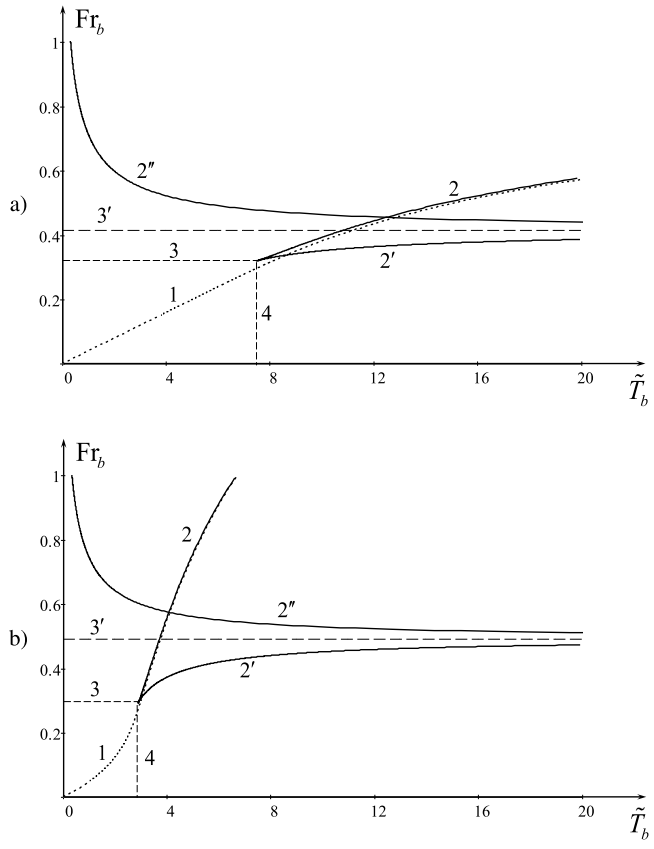

FIG. 8. The critical Froude number against the normalised wave period $\tilde{T}_b$ for gravity-capillary surface waves with $S = 7.4 \times 10^{-3}$. Frame (a) pertains to $\Omega = 0$, and frame (b)—to $\Omega = 1$.

E. A specific case of wave blocking

Consider now wave transformation at the blocking point when the frequency ω_0 of the counter-current propagating wavetrain is such that at the blocking point the local maximum of the dispersion curve in the left half-plane of Fig. 5 is lower than the local maximum of the dispersion curve in the right half-plane of that figure. This situation is depicted in Fig. 9(a).

The counter-current propagating gravity wave with a relatively small wave number in absolute value (see dot on line 1 in Fig. 9(b)) gradually changes so that its wave number increases in absolute value (see dots on lines 2 and 3_0 in Fig. 9(b)). When the wave train attains the position where the dispersion curve has a maximum at $\tilde{\omega} = \tilde{\omega}_0$ (see lines 3_0 and 3a), it experiences a transformation into the other modes. The reflected gravity-capillary wave arises on the dispersion curve 3a close to the maximum of the curve, but on the left. This is a wave of positive energy having positive group velocity (its energy flux directed to the right), but negative phase velocity. In the course of propagation, its wave number increases in absolute value.

In addition to that, four other waves arise at the blocking point. One of these is a transmitted capillary wave (see the very left dot on line 3b in Fig. 9(a)). This is a wave of positive energy having negative group and phase velocities. In the course of propagation, its wave number increases in absolute value. Another is the reflected gravity wave (see dot on line 0 in Fig. 9(b)). This is also a wave of a positive energy having positive group and phase velocities. Its wave number increases during the course of propagation as the dispersion curve 0 inclines to the right with decreasing Froude number.

Two other waves arising at the blocking point are negative energy waves; they are shown in Fig. 9(a) by dots on lines 3″a and 3″b. They have positive phase velocities, but their group velocities

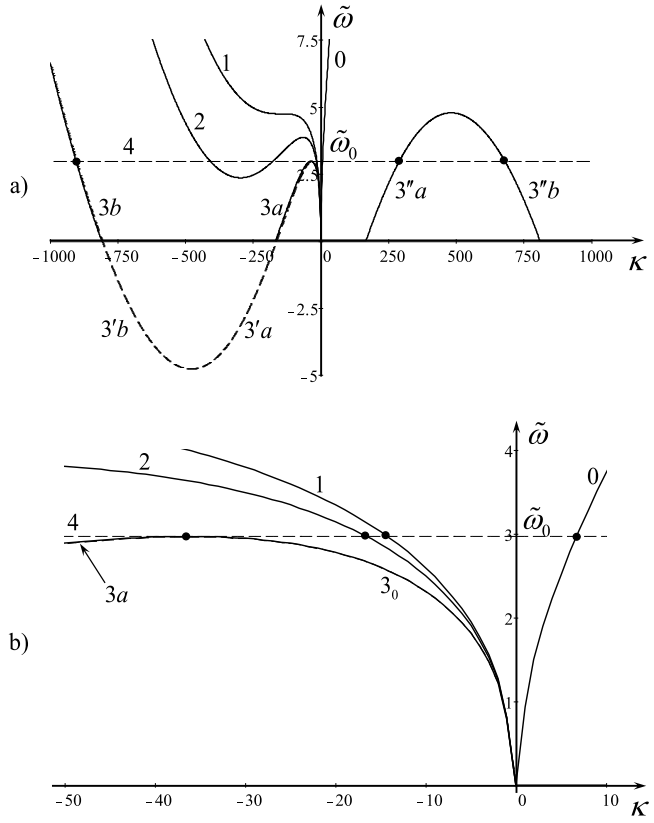

FIG. 9. The dispersion relation as per Eq. (2) with $\Omega = 0$ and $S = 7.4 \times 10^{-6}$. Lines 0 and 1 pertain to co- and counter-current propagating waves, respectively, when $Fr = 5.67 \times 10^{-2}$, line 2 pertains to counter-current propagating waves when $Fr = 6.67 \times 10^{-2}$, line 3_0 pertains to counter-current propagating waves, line 3a to co-current propagating waves when $Fr = 8.5 \times 10^{-2}$. Panel (b) shows the magnified fragment of panel (a). Horizontal dashed line 4 depicts the frequency $\tilde{\omega}_0$ of the initial wavetrain travelling against the current. Lines 3″a and 3″b are counterparts of lines 3′a and 3′b, respectively, for positive frequencies and wavenumbers.

are opposite. The wave on the dispersion branch 3″a has positive group velocity, and its wave number increases in the course of propagation as the local maximum of the dispersion curve decreases in the direction of the current. And the wave on the dispersion branch 3″b has negative group velocity, and its wave number increases too in the course of propagation as the local maximum of the dispersion curve increases when the wave propagates against the current.

Two of these four reflected waves can experience the secondary transformation at other blocking points. Consider first the reflected gravity-capillary wave on the dispersion branch 3a. When it propagates downstream, the dispersion curve gradually rises up and eventually it becomes similar to curve 2 shown in Fig. 9(a). The blocking point occurs where the minimum of the dispersion line becomes equal to the wave frequency $\tilde{\omega}_0$. Two reflected waves arise at this point. One is a capillary wave on the dispersion branch 3b and the other is a gravity wave on branch 3_0 shown in Fig. 9(b); both are PEWs propagating to the left with negative group and phase velocities. A transmitted gravity wave also arises on the dispersion branch 0. This wave propagates to the right having positive energy and positive group and phase velocities. Finally, two NEWs arise on the dispersion branches $3''a$ and $3''b$.

One of the two NEWs, namely, the wave on the dispersion branch $3''a$ can also experience a secondary blocking when the maximum of the dispersion curve becomes equal to the wave frequency $\tilde{\omega}_0$. Again the variety of waves appear due to transformation of the wave arriving at the blocking point. We will not describe them in detail any more, but we only notice that the details of the wave transformation have not been studied thus far. This remains a challenging and interesting problem, especially when NEWs participate in the transformation. One may expect the onset of

wave instabilities due to linkage between the positive and negative energy waves at the blocking point (see, e.g., Refs. 35 and 36). In this paper we only present a qualitative description of possible effects associated with wave blocking in the presence of surface tension when NEWs may appear. A complete description of wave transformation requires further development including accounting for nonlinear effects; this is, however, beyond the scope of the present work.

IV. THE BLOCKING PHENOMENON OF PURE CAPILLARY WAVES ON A SHEAR CURRENT WITH CONSTANT VORTICITY

It is of interest to study the peculiarities of the blocking phenomenon for pure capillary waves. Such a situation may arise when the gravity effect is negligible, e.g., in the state of weightlessness, or when the effect of surface tension is made artificially very strong in comparison with the gravity effect. Considering such a case, we put $g = 0$ in Eq. (1) and using now another normalisation for the frequency $\tilde{\omega} = \omega\sqrt{\rho h^3/\sigma}$, but the same normalisation for the wave number $\kappa = kh$ as before, we present the dispersion relation in dimensionless form

$$\tilde{\omega}^{\pm}(\kappa) = \left(\hat{\mathbf{U}}_0 \cdot \hat{\mathbf{k}}_0\right)(\mathrm{Fs}|\kappa| - \Omega_s \tanh|\kappa|) + \sqrt{(\Omega_s \tanh|\kappa|)^2 + |\kappa|^3 \tanh|\kappa|}, \tag{31}$$

where $\mathrm{Fs} = U_0\sqrt{h\sigma}$ is the capillary analog of the Froude number, and $\Omega_s = (\alpha h/2)\sqrt{h/\sigma}$ is the parameter characterising the vorticity of the background flow. Dispersion curves are shown in Fig. 10 for different values of the Froude number and vorticity parameter. Notice that the vorticity parameter can be presented in the form $\Omega_s = (h/l_\alpha)^{3/2}$, where $l_\alpha = \sqrt[3]{4\sigma/\rho\alpha^2}$ is the characteristic length scale associated with the vorticity and surface tension.

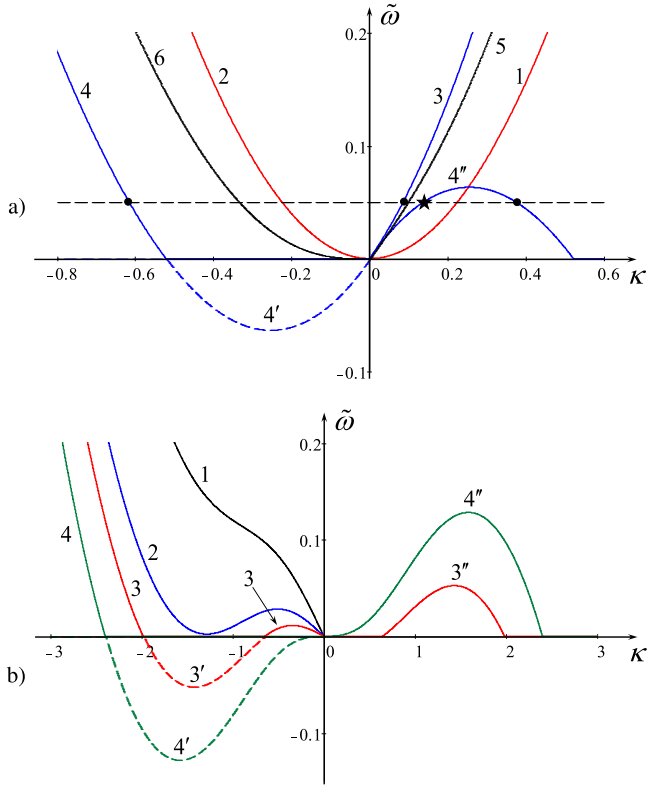

FIG. 10. Dispersion curves as per Eq. (31). In frame (a) lines 1 and 2 pertain to the case when $\mathrm{Fs} = \Omega_s = 0$; lines 3, 4, 4′, and 4″ pertain to the case when $\mathrm{Fs} = 0.5$ and $\Omega_s = 0$; lines 5 and 6 pertain to the case when $\mathrm{Fs} = 0.5$ and $\Omega_s = \mathrm{Fs}/2$. In frame (b) $\Omega_s = 1 > \Omega_{cr}$; line 1 pertains to $\mathrm{Fs} = 1.8$, line 2—to $\mathrm{Fs} = 1.91$; lines 3, 3′, and 3″—to $\mathrm{Fs} = 1.95$; and lines 4, 4′, and 4″—to $\mathrm{Fs} = 2$. The dispersion branches corresponding to the co-current propagating waves are similar to lines 1, 3, and 5 in frame (a) and are not shown here.

Without a current, the two branches of the dispersion curve, $\tilde{\omega}^+$ and $\tilde{\omega}^-$, are symmetrical with respect to the vertical axis as shown in Fig. 10(a) (see lines 1 and 2). In the presence of a *non-vortical* current ($\Omega_s = 0$) they become non-symmetrical. Line 1 in Fig. 10(a) transfers to line 3, and line 2 splits into lines 4 and 4″, where line 4″ is the reflection of line 4′; it corresponds to NEWs.

In such a flow the counter-current propagating waves do not experience a blocking. The blocking phenomenon can occur only for co-current propagating NEWs that correspond to the portion of the dispersion curve 4″ which is to the left of the maximum (see, e.g., the star on line 4″). These waves have positive group velocities and travel in the direction where the background current gradually decreases. Therefore the maximum of the dispersion curve 4″ diminishes, the carrier wavenumber slightly increases, and the wave blocking phenomenon eventually occurs at some point. At this point one positive energy wave (the transmitted wave) appears on branch 3 and two reflected waves appear, one on branch 4 (PEW) and another on branch 4″ (NEW) (see dot on the right of the maximum). Both of these waves have negative group velocity; therefore, they propagate against the flow with gradually increasing wavenumbers.

In the presence of relatively small vorticity ($\Omega_s < \mathrm{Fs}/2$) the qualitative character of the dispersion relation remains the same as described above, but the positions of minima (like in line 4′) and maxima (like in line 4″) shift closer to zero. When the vorticity parameter Ω_s becomes equal to Fs/2, then the minimum and maximum completely disappear (see lines 5 and 6 in Fig. 10(a)), and the blocking phenomenon becomes impossible. Therefore, we can conclude that the effect of vorticity prevents the blocking phenomenon. This remains true for even higher values of vorticity until it reaches some critical value Ω_{cr}; after that the character of the dispersion curve changes qualitatively, as shown in Fig. 10(b) (see lines 4).

The critical value of the vorticity can be found explicitly in the long-wave approximation ($|\kappa| \ll 1$), when the dispersion relation for $\tilde{\omega}^-$ reads

$$\tilde{\omega}^- \approx (2\Omega_s - \mathrm{Fs})\kappa + \frac{3 - 4\Omega_s^2}{6\Omega_s}\kappa^3. \tag{32}$$

Finding then the extrema, we obtain after differentiation with respect to κ,

$$\kappa_c(\mathrm{Fs}, \Omega_s) = -\sqrt{\frac{2\Omega_s(\mathrm{Fs} - 2\Omega_s)}{3 - 4\Omega_s^2}}, \quad \tilde{\omega}_c^-(\mathrm{Fs}, \Omega_s) = \frac{2}{3}(\mathrm{Fs} - 2\Omega_s)\sqrt{\frac{2\Omega_s(\mathrm{Fs} - 2\Omega_s)}{3 - 4\Omega_s^2}}, \tag{33}$$

where κ_c and $\tilde{\omega}_c^-$ are the wavenumber and frequency, respectively, at the critical point.

From these formulae one can see that the critical value of Ω_s in the long-wave approximation is $\Omega_{cr} = \sqrt{3}/2$. In general, beyond the long-wave approximation, the critical value of Ω_s can be found from a transcendental equation which is not presented here. For $\Omega_s > \Omega_{cr}$ the dispersion curves are shown in Fig. 10(b); they are qualitatively similar to what is shown in Fig. 9.

It is interesting to note that, for a shear flow with constant vorticity, NEWs can appear even in the absence of the blocking phenomenon when the dispersion curve is monotonic. As follows from the analysis presented in our paper,[31] the condition for existence of NEWs in the case when there is no gravity reads

$$\mathrm{Fs} > \Omega_s \frac{\tanh|\kappa|}{|\kappa|} + \frac{\kappa^2 \tanh|\kappa|}{\sqrt{(\Omega_s \tanh|\kappa|)^2 + |\kappa|^3 \tanh|\kappa|}}. \tag{34}$$

The frequency of the zero-energy wave is

$$\tilde{\omega}_0 = \frac{(\Omega_s \tanh|\kappa|)^2}{\sqrt{(\Omega_s \tanh|\kappa|)^2 + |\kappa|^3 \tanh|\kappa|}}, \tag{35}$$

where for given Fs and Ω_s, κ should be determined from the solution of Eq. (34) with the two sides set equal.

The condition for the blocking phenomenon can be readily derived from Eq. (31) using the condition $\tilde{c}_g \equiv d\tilde{\omega}_2/d\kappa = 0$. The dependence of the wave frequency $\tilde{\omega}^-$ at the blocking point on the modified Froude number, $\tilde{\omega}_b(\mathrm{Fs}_b)$, can be presented in parametric form. When $\Omega_s = 0$ the formulae read

$$\tilde{\omega}_b(\kappa,0) = \frac{|\kappa|}{2}\sqrt{\frac{|\kappa|}{\tanh|\kappa|}}\left[\tanh|\kappa| + |\kappa|\left(1-\tanh^2\kappa\right)\right], \tag{36}$$

$$\mathrm{Fs}_b(\kappa,0) = \frac{1}{2}\sqrt{\frac{|\kappa|}{\tanh|\kappa|}}\left[3\tanh|\kappa| + |\kappa|\left(1-\tanh^2\kappa\right)\right]. \tag{37}$$

In the general case, when $\Omega_s \neq 0$, the formulae are more complicated,

$$\tilde{\omega}_b(\kappa,\Omega_s) = \frac{\left(|\kappa| - \tanh|\kappa| - |\kappa|\tanh^2|\kappa|\right)\left(|\kappa|^3 + 2\Omega_s^2\tanh|\kappa|\right) + 2|\kappa|^3\tanh|\kappa|}{2\sqrt{\tanh|\kappa|\left(|\kappa|^3 + \Omega_s^2\tanh|\kappa|\right)}} +$$

$$\Omega_s\left(|\kappa| - \tanh|\kappa| - |\kappa|\tanh^2|\kappa|\right), \tag{38}$$

$$\mathrm{Fs}_b(\kappa,\Omega_s) = \frac{\left(2\Omega_s^2\tanh|\kappa| + |\kappa|^3\right)\left(1-\tanh^2|\kappa|\right) + 3\kappa^2\tanh|\kappa|}{2\sqrt{\tanh|\kappa|\left(|\kappa|^3 + \Omega_s^2\tanh|\kappa|\right)}} + \Omega_s\left(1-\tanh^2|\kappa|\right). \tag{39}$$

The relationship between $\tilde{\omega}_b^-$ and Fs_b can be presented in terms of the parametric dependence of the critical Froude number on the normalized wave period $\mathrm{Fs}_b\left(\tilde{T}_b\right)$, where $\tilde{T}_b = T_b\sqrt{\sigma/h^3}$. This dependence is plotted in Fig. 11(a) for three values of $\Omega_s = 0, 0.5$, and 1 (cf. Fig. 8).

Line 1 in this figure pertains to the case of surface capillary waves on a uniform flow with zero vorticity $\Omega_s = 0$. Line 2 pertains to the case of surface capillary waves on a shear flow with constant vorticity, less than the critical value $\Omega_s = 0.5 < \Omega_{cr}$. Lines 3, 3′, and 3″ pertain to the case of surface capillary waves on a shear flow with constant vorticity, greater than the critical

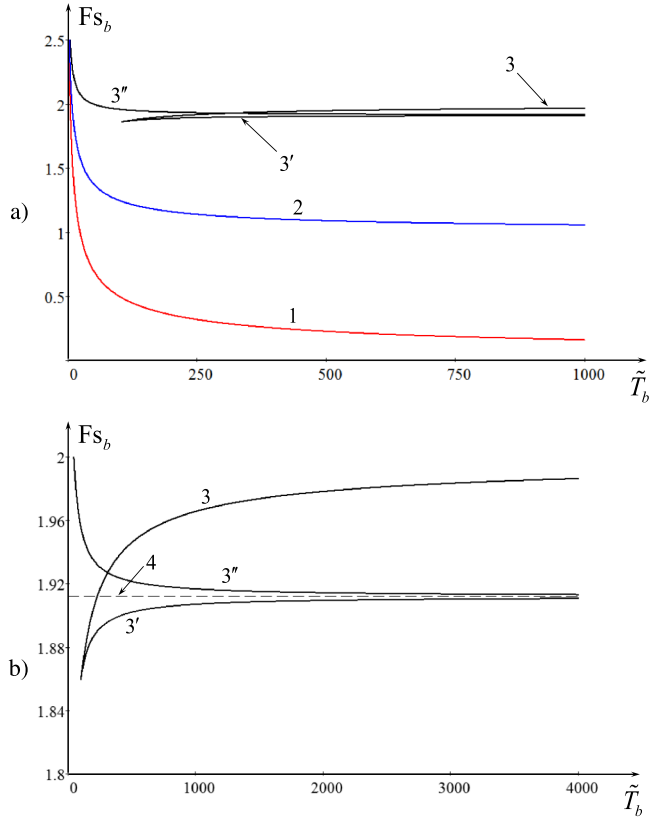

FIG. 11. The critical Froude number against the normalised wave period $\tilde{T}_b$ for capillary surface waves on a linear shear flow. In frame (a) line 1 pertains to $\Omega = 0$, line 2 pertains to $\Omega = 0.5$, and lines 3, 3′, and 3″ pertain to $\Omega_s = 1 > \Omega_{cr}$. Frame (b) represents a magnified fragment of frame (a) where one can clearly see lines 3, 3′, and 3″ which pertain to $\Omega_s = 1$. Line 4 in this frame shows the asymptotic value of the Froude number when $\tilde{T}_b(\kappa,\Omega_s) \to \infty$.

value $\Omega_s = 1 > \Omega_{cr}$. Branch 3 describes the dependence of the critical Froude number on the wave period for the first blocking point, which corresponds to the maximum of PEWs on the dispersion curve (see the maximum on curve 2 in Fig. 10(b)). This line asymptotically approaches $2\Omega_s$ when $\tilde{T}_b \to \infty$.

Line 3′ depicts the dependence of the critical Froude number on the wave period for the second blocking point which corresponds to the minimum of PEWs on the dispersion curve (see the minimum on curve 2 in Fig. 10(b)). This line asymptotically approaches (when $\tilde{T}_b \to \infty$) dashed horizontal line 4, where $\mathrm{Fs}_b = 2\sqrt[3]{\Omega_s}$. In the dimensional variables the dependence between Fs_b and Ω_s reads $U_{\alpha\sigma} = \sqrt[3]{4\alpha\sigma}$.

Line 3″ depicts the dependence of the critical Froude number on the wave period for the third blocking point which corresponds to the maximum of NEWs on the dispersion curve (see the maximum on curve 3″ in Fig. 10).

Thus, we can see again that the effect of vorticity on surface capillary waves, to a certain extent, is similar to the effect of gravity on gravity-capillary waves with the vorticity playing the role of an effective gravity field. This is reflected in the qualitative similarity between Figs. 8 and 11.

V. CONCLUSION

In this paper, on the basis of the analysis of dispersion properties of surface waves, we studied the peculiarities of the blocking phenomenon in a shear flow gradually varying in a horizontal direction. The flow can be uniform with depth or linearly varying. In the former case, gravity waves of any period can be blocked at a certain critical speed of the current, whereas in the latter case, the higher the wave period, the higher surface speed is required to block the wave.

When the surface tension is taken into account, the problem becomes more complicated as gravity-capillary waves may experience multiple reflections at separate blocking points. Such a phenomenon has been experimentally observed and confirmed in numerical study.[1,28,41] Here we have calculated the relationships between the wave periods and Froude numbers at the blocking points and described in detail the kinematics of the blocking phenomenon.

We have also considered (for the first time) the specific case of a blocking phenomenon which can occur in the absence of gravity. It has been shown that in this case the effect of vorticity on surface capillary waves is similar to the effect of gravity on gravity-capillary waves. The corresponding diagrams presented in Figs. 8 and 11 look very similar to each other.

The results obtained provide good insight into the problem and may allow us to develop a nonlinear theory of the wave blocking phenomenon, as well as to validate the predicted effects in experiments and/or in numerical modelling.

ACKNOWLEDGMENTS

This work was initiated when one of the authors (Y.S.) visited the Laboratory J.-A. Dieudonné of the University of Nice in January–February 2011 and it was completed when Y.S. visited Institut Pprime, Université de Poitiers in January–February 2014 and in July–December 2015. Y.S. is grateful to both Universities and Région Poitou-Charentes for the invitations and hospitality. This research was supported by the University of Poitiers (ACI UP on Wave-Current Interactions 2013-2014). The French National Research Agency (ANR) funds the current work through the grant HARALAB (No. ANR-15-CE30-0017-04). The authors are indebted to Scott Robertson for his help in the manuscript preparation for publication.

[1] S. I. Badulin, K. V. Pokazeyev, and A. D. Rozenberg, "A laboratory study of the transformation of regular gravity-capillary waves in inhomogeneous flows," Izv. Atmos. Oceanic Phys. **19**(10), 782–787 (1983).
[2] T. B. Benjamin, "The threefold classification of unstable disturbances in flexible surfaces bounding inviscid flows," J. Fluid Mech. **16**, 436–450 (1963).
[3] F. Biesel, "Etude théorique de la houle en eau courante," Houille Blanche **5**, 279–285 (1950).
[4] I. Brevik, "The stopping of linear gravity waves in currents of uniform vorticity," Phys. Norv. **8**, 157–162 (1976).
[5] J. C. Burns, "Long waves in running water," Proc. Cambridge Philos. Soc. **49**, 695–705 (1953).
[6] R. A. Cairns, "The role of negative energy waves in some instabilities of parallel flows," J. Fluid Mech. **92**, 1–14 (1979).

[7] W. Choi, "Nonlinear surface waves interacting with a linear shear current," Math. Comput. Simul. **80**, 29–36 (2009).
[8] M. W. Dingemans, *Water Wave Propagation Over Uneven Bottoms* (World Scientific, 1997).
[9] S. A. Ellingsen and I. Brevik, "How linear surface waves are affected by a current with constant vorticity," Eur. J. Phys. **35**, 025005 (2014).
[10] J. D. Fenton, "Some results for surface gravity waves on shear flows," J. Inst. Math. Its Appl. **12**, 1–20 (1973).
[11] T. S. Hedges, "Combinations of waves and currents: An introduction," Proc. - Inst. Civ. Eng. **82**, 567–585 (1987).
[12] I. G. Jonsson, "Wave-current interactions," in *The Sea*, edited by B. Le Mehaute and D. M. Hanes (John Wiley, 1990), pp. 65–120.
[13] I. Kantardgi, "Effect of depth current profile on wave parameters," Coastal Eng. **26**(3–4), 195–206 (1995).
[14] I. G. Kantarzhi, I. L. Makarova, and Ye. N. Pelinovskiy, "Wave transformation by a current having linear velocity shear with depth," Oceanology **29**(2), 145–150 (1989).
[15] B. B. Kadomtsev, A. B. Mikhailovskii, and A. V. Timofeev, "Negative energy waves in dispersive media," Sov. Phys. JETP **47**, 2267–2269 (1964).
[16] P. Karageorgis, "Dispersion relation for water waves with non-constant vorticity," Eur. J. Mech. B: Fluids **34**, 7–12 (2012).
[17] J. T. Kirby and T. M. Chen, "Surface waves on vertically sheared flows: Approximate dispersion relations," J. Geophys. Res. **94**, 1013–1027, doi:10.1029/JC094iC01p01013 (1989).
[18] Ch. Kharif, E. Pelinovsky, and A. Slunyaev, *Rogue Waves in the Ocean* (Springer, 2009), p. 216.
[19] L. D. Landau and E. M. Lifshitz, *Hydrodynamics. Course of Theoretical Physics*, 5th ed. (Fizmatlit, Moscow, 2006), Vol. 6 (in Russian) [English translation: *Fluid Mechanics*, 2nd ed. (Pergamon Press, Oxford, 1987)].
[20] I. Lavrenov, *Wind-Waves in Oceans* (Springer, 2003).
[21] H. Margaretha, "Mathematical modelling of wave-current interaction in a hydrodynamic laboratory basin," Ph.D. dissertation, University of Twente, Enschede, The Netherlands, 2005.
[22] A. B. Mikhailovskii, *Theory of Plasma Instabilities, V. 1 (1975)*, 2nd ed. (Atomizdat, Moscow, 1977), Vol. 2 (in Russian) [English version: Consultants Bureau, NY, 1974].
[23] J.-C. Nardin, G. Rousseaux, and P. Coullet, "Wave-current interaction as a spatial dynamical system: Analogies with rainbow and black hole physics," Phys. Rev. Lett. **102**(12), 124504 (2009).
[24] H. M. Nepf and S. G. Monismith, "Wave-dispersion on a sheared current," Appl. Ocean. Res. **16**(5), 313–315 (1994).
[25] M. V. Nezlin, "Negative-energy waves and the anomalous Doppler effect," Sov. Phys. Usp. **19**, 946–954 (1976).
[26] L. A. Ostrovsky, S. A. Rybak, and L. Sh. Tsimring, "Negative energy waves in hydrodynamics," Sov. Phys. Usp. **29**(11), 1040–1052 (1986).
[27] D. H. Peregrine, "Interaction of water waves and currents," Adv. Appl. Mech. **16**, 9–117 (1976).
[28] K. V. Pokazeyev and A. D. Rozenberg, "Laboratory studies of regular gravity-capillary waves in currents," Okeanologiya **23**(4), 429–435 (1983).
[29] A. K. Pramanik, "Capillary-gravity waves produced by a moving pressure distribution," ZAMP **31**, 174–180 (1980).
[30] G. Rousseaux, P. Maïssa, C. Mathis, P. Coullet, T. G. Philbin, and U. Leonhardt, "Horizon effects with surface waves on moving water," New J. Phys. **12**, 095018 (2010).
[31] P. Maïssa, G. Rousseaux, and Y. Stepanyants, "Negative energy waves in shear flow with a linear profile," Eur. J. Mech. B: Fluids **56**, 192–199 (2016).
[32] V. I. Shrira, "On the sub-surface waves of the mixed layer of the upper ocean," Dokl. Akad. Nauk SSSR **308**, 732–736 (1989) [English translation: "On the sub-surface waves of the mixed layer of the upper ocean," Doklady USSR Acad. Sci. **308**, 276–279 (1989)].
[33] J.-H. Shyu and O. M. Phillips, "The blockage of gravity and capillary waves by longer waves and currents," J. Fluid Mech. **217**, 115–141 (1990).
[34] R. A. Skop, "Approximated dispersion relation for wave-current interactions," J. Waterw., Port, Coastal, Ocean Eng. **113**, 187–195 (1987).
[35] Yu. A. Stepanyants and A. L. Fabrikant, "Propagation of waves in hydrodynamic shear flows," Sov. Phys. Usp. **32**(9), 783–805 (1989).
[36] Yu. A. Stepanyants and A. L. Fabrikant, *Propagation of Waves in Shear Flows* (Nauka Fizmatlit, Moscow, 1992) (in Russian) [English version: (World Scientific, Singapore, 1998)].
[37] C. Swan and R. L. James, "A simple analytical model for surface water waves on a depth-varying current," Appl. Ocean Res. **22**, 331–347 (2001).
[38] G. I. Taylor, "The action of a surface current as a breakwater," Proc. R. Soc. A **231**, 466–478 (1955).
[39] G. P. Thomas and G. Klopman, "Wave-current interactions in the nearshore region," in *Gravity Waves in Water of Finite Depth*, edited by J. N. Hunt, Advances in Fluid Mechanics (CMP, Southampton, 1997), Vol. 10.
[40] P. D. Thompson, "The propagation of small surface disturbance through rotational flow," Ann. N. Y. Acad. Sci. **5**, 463–474 (1949).
[41] K. Trulsen and C. C. Mei, "Double reflection of capillarylgravity waves by a non-uniform current: A boundary-layer theory," J. Fluid Mech. **251**, 239–271 (1993).
[42] S. Tsao, "Behaviour of surface waves on linearly varying currents," J. Geophys. Res. **79**, 4498–4508 (1957).
[43] E. Wahlen, "On rotational water waves with surface tension," Philos. Trans. R. Soc., A **365**, 2215–2225 (2007).